JACS
JOURNAL OF THE AMERICAN CHEMICAL SOCIETY

Article

pubs.acs.org/JACS

A Two-Dimensional Polymer Synthesized through Topochemical [2 + 2]-Cycloaddition on the Multigram Scale

Ralph Z. Lange,[†] Gregor Hofer,[†,‡] Thomas Weber,[‡] and A. Dieter Schlüter*[,†]

[†]Institute of Polymers and [‡]X-ray Platform, Department of Materials, Swiss Federal Institute of Technology, ETH Zürich, Vladimir Prelog-Weg 5, 8093 Zürich, Switzerland

Supporting Information

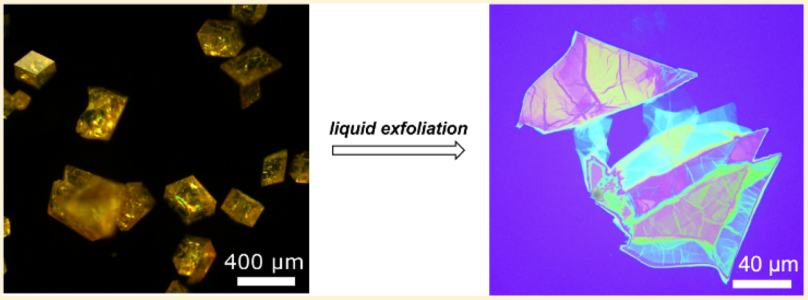

ABSTRACT: The single-crystal-to-single-crystal (scsc) synthesis of a 2D polymer based on photochemically triggered [2 + 2]-cycloaddition is reported. Both monomer and polymer single crystals are analyzed by X-ray diffraction, which is the first case of a scsc two-dimensional polymerization based on this cycloaddition and the third ever case for a scsc synthesis of a 2D polymer. The product crystals at quantitative conversion are wet-exfoliated under mild conditions and afford countless features that are single and double layers as judged by their AFM heights of $h_{AFM} \approx 1.2 \pm 0.5$ and 2.2 ± 0.5 nm, respectively. The X-ray-structure-based molecular weight of the 2D polymers and their degree of polymerization per μm^2 are M = 360 MDa and P_n = 464 900, respectively. The sheet size is on the order of 5×5 μm^2.

INTRODUCTION

Currently, there is vigorous research activity toward the creation of novel two-dimensional (2D) materials.[1] It is expected that by making them, applications will be discovered that are complementary to what 3D materials already offer. Possible utilizations include membranes, coatings, blends, and organic electronics.[1b,2] Two-dimensional materials such as metal−organic frameworks (2D MOF)[3] are in the realm of inorganic and materials chemistry, while the covalent organic frameworks (2D COF),[4] the covalent triazine frameworks (CTF),[5] and even more so the 2D polymers[6] are at the heart of organic chemistry. We recently proposed 2D polymers to be sheetlike entities meeting the following five criteria: topological planarity, crystallinity (existence of planar repeat units), covalent bonding, monolayer thickness, and separability.[7] Related as well as different views of what the term "2D polymer" should refer to have also been proposed.[8] Concrete examples of 2D polymers based on topochemical syntheses in the single crystal were reported and are substantiated by proof of structure based on single-crystal X-ray diffraction (XRD).[9] Other crystal approaches have also been reported.[10] Additionally, there were interesting cases of 2D materials that are related to 2D polymers in that at least some of the criteria are met while other criteria await to be proven. They were created by different approaches, ranging from syntheses at the air/water[11] and liquid/liquid interfaces[12] all the way to on-surface[13] and in-solution chemistry.[14] The chemistries that so far led to success in the single-crystal approach are mostly photochemically induced [4 + 4]-cycloadditions of anthracenes and [4 + 2]-cycloadditions of anthracenes and acetylenes.[9,10a−c] They were applied to monomers properly packed in layers such that the reactive groups of nearest neighbors are exposed to one another in the required arrangement. In the beginning of what is likely to develop into a larger field of research,[15] it is of utmost importance to broaden the structural foundation. This is why we and others focus our efforts on discovering chemistries and procedures leading to novel 2D polymers. In light of the first breakthroughs, aspects such as simplicity and costs will turn increasingly more important. Given the considerable complexity the structure elucidation of a monolayer sheet inevitably involves, the discovery process currently is directed toward the creation of 2D polymers in single crystalline form. Although the exfoliation of single crystals has been proven to be tedious,[16] it has the invaluable benefit that structure analytics can be supported by single-crystal XRD which, among others, facilitates the acceptance of 2D polymers as a reality.

Topochemical reactions have been studied in detail. Linear polymerizations within single crystals date back to the 1970s, when Wegner and Hasegawa polymerized, for example, distyrylpyrazines and diacetylenes, respectively, to the corresponding macromolecules.[17] Topochemical olefin dimeriza-

Received: November 25, 2016
Published: January 13, 2017

DOI: 10.1021/jacs.6b11857
J. Am. Chem. Soc. 2017, 139, 2053−2059

tion,[18] as used in the case of 2,5-distyrylpyrazine (DSP), is not only attractive for the creation of linear polymers from diolefinic monomers but potentially also for 2D polymerization, given that properly chosen triolefinic monomers are employed.

A first indication of the feasibility was recently published by Wang et al.,[10c] but unfortunately, the reaction led to crystal disassembly, which prevented proof of the polymer structure by XRD. Steering the packing of a monomer, such that it polymerizes in the desired fashion, is challenging, even after so many years of crystal engineering.[19,20] While there is some knowledge on favored packing motifs, trial and error remains an important ingredient. It is thus attractive when the choice of solvent and the methods of crystallization are not the only factors to influence the packing of an organic compound. Interestingly, Novak et al. investigated the topochemical dimerization of styryl pyrylium salts **1** (Figure 1a) to give the

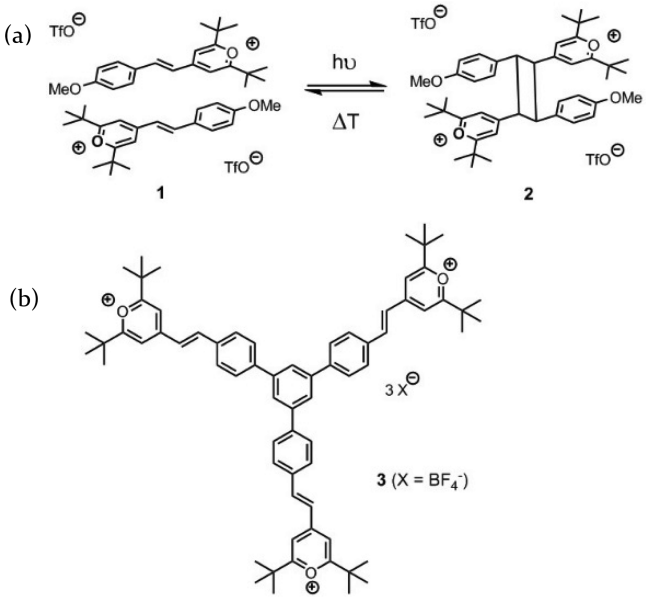

Figure 1. (a) Dimerization of the styryl pyrylium salt **1** to the cyclobutane derivative **2** as model for a topochemical polymerization. (b) Structure of the monomer **3**.

head-to-tail cyclobutanes **2** for a number of counterions.[21] Without any synthesis effort, this allowed the creation of a whole variety of single crystals, some of which had the two neighboring olefins in a geometry that allowed photochemically induced dimerizations. We considered this advantage when designing monomer **3**.

We here report an easy, inexpensive, and 35 g scale synthesis of the pyrylium-based triolefinic monomer **3** ($X = BF_4^-$) and its crystallization into batches up to 5 g of layered single crystals with all the edge lengths being similar and up to 5 mm. Further, we will discuss how the packing of the monomer enables the formation of a novel 2D polymer by photoirradiation on the same scale. The crystals stay intact during polymerization, allowing us to prove the polymer structure by in-house XRD. The new 2D polymer structure is further supported by IR and ^{13}C CP/MAS solid-state NMR spectroscopy. Additionally, we will explain that this novel single-crystal-to-single-crystal (scsc) transformation is associated with an improved mechanical stability of the otherwise sensitive crystals. Further, we will describe the wet exfoliation of the completely polymerized single crystals, which results in a large number of thin objects. We believe these objects to be single- and double-layer 2D polymer sheets based on AFM height determination. Finally, we will show that the polymerization is thermally reversible at around 150 °C. While this temperature is high enough to not affect the wet exfoliation at room temperature, it is low enough to open up interesting future opportunities for laser cutting of sheets associated with a clean chemical process.

RESULTS AND DISCUSSION

The light-mediated dimerization of 2,6-di(*tert*-butyl)styryl pyrylium salts **1** was first described by Hesse and Hünig in 1985 (Figure 1).[22] The mechanistic details of this reaction were later revealed by Novak et al. on the basis of comprehensive crystallographic studies.[23] Inspired by this, we designed monomer **3** and set out to synthesize it in a straightforward fashion. Scheme S1 of the Supporting Information (SI) shows the synthetic sequence by which monomer **3** was obtained in batches of up to 35 g in only four steps from commercially available, inexpensive starting materials. The absence of chromatographic purification and the choice of the solvents should enable a technical scale application. Monomer **3** was purified by recrystallization from a mixture of acetic and formic acids.

The best monomer crystals in terms of crystal size and quality of Bragg reflections (narrow full width at half-maximum) were obtained by controlled cooling of saturated solutions of **3** in methanol/acetonitrile mixtures over a time of 1−5 d (Figure S1, SI). In more than 100 crystallizations we found that cooling beyond 1 d yielded crystals whose edge lengths ranged between 100 μm and 5 mm. Efforts to target crystals with distinct sizes were met with difficulties. All analytical procedures described in this paper, including XRD, refer to crystals that had an average edge length of approximately 500 μm. Figure S2 (SI) provides optical microscopy (OM) images and a photograph illustrating the whole size range typically obtained.

The monomer crystals turned out to be sensitive. They needed to be either covered by the mother liquor or exposed to solvent atmosphere (by residual mother liquor present in the sealed vial). Also, when touching the crystals with a spatula, they disintegrate into a viscous microcrystalline mass. The handling of the crystals in particular regarding mounting in the diffractometer was facilitated by polymerizing the monomer crystals to low conversion (<25%).[24] Minor features of the monomer crystal structure could not be solved with sufficient accuracy; in particular, diastereochemical arrangements were troublesome. However, these missing details could be clarified on the basis of the polymer crystal structure. Reciprocal space reconstructions and different views of the packing within the monomer crystals are displayed in Figures S3−S5 (SI). The monomers arrange themselves into layers [three per unit cell (Figure 2a)], whereby in each layer the olefins of neighboring monomers are mutually positioned such that dimerization can take place. Thus, the Schmidt criterion for topochemical reaction is fully met for the olefin pairs within a layer (olefin−olefin distances, 3.9 Å each; Figure 2b, left),[25] while the distance between olefins belonging to different layers is so large (shortest olefin−olefin distances, 7.66 Å; Figure 2b, right) that an interlayer reaction should be kinetically hindered.

This kinetic hindrance restricts the polymerization to intralayer instead of interlayer dimerizations and thus is the key to obtaining 2D polymers. Interestingly, monomer **3**

DOI: 10.1021/jacs.6b11857
J. Am. Chem. Soc. 2017, 139, 2053−2059

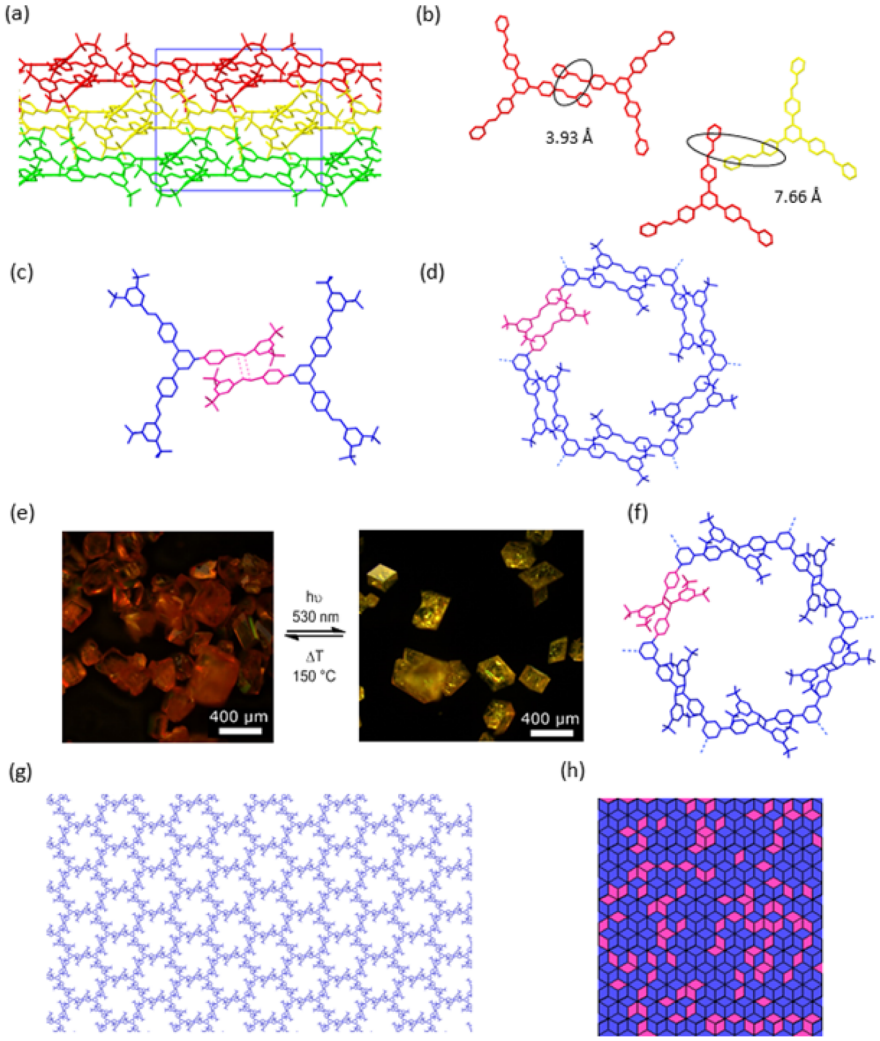

Figure 2. Scsc transformation of monomer **3** to the corresponding 2D polymer. (a) The three layers (red, yellow, green) per unit cell the monomer crystal is composed of. (b) Olefin−olefin distances of nearest neighbor olefins within the same layer (red) and between neighboring layers (red/yellow). (c) The three olefins of monomer **3** are turned either all in the same orientation relative to the core (not shown) or two in the same orientation (blue) and the remaining one turned by roughly 180° (purple). The ratio is approximately 5:1. (d) Arrangement of six monomers within a layer, which upon polymerization will turn into the rim of a pore of the 2D polymer. One pair of olefins is presented in the less frequent relative conformation (purple), while all others are presented in the most frequent relative conformation. On average, each such arrangement has one such stereochemical irregularity. (e) Optical microscopy images of small crystals of monomer and polymer illustrating the color change associated with the topochemical reaction. (f) Structure of a pore of the 2D polymer showing one diastereomeric repeating unit, which is a consequence of the olefin orientations in the monomer crystal (blue, major distereomer; purple, minor) (g) Structure of a 2D polymer sheet in the crystal obtained from monomer **3** with layer group $p\bar{3}$. The pores are filled by not-resolved solvent molecules, which are omitted for clarity. This representation is idealized in that all cyclobutanes formed show the same stereochemistry, although approximately 16% of their diastereomeric forms are presumably randomly distributed over the sheet (on average one diastereomer per pore). (h) Schematic representation of a random distribution of the diastereomers in a single sheet of the 2D polymer according to the 5:1 ratio.

assumes different conformations concerning the orientations of each of its three arms.

Figure 2c shows one of the four conformational isomers possible for two adjacent monomers in the crystal. Two of the three arms emanating from the core present their olefins in the same orientation (blue part of the structure in Figure 2c) and the remaining arm is turned relative to the other two by roughly 180° (purple part of the same image). Although the ratio of two diastereomers is 5:1, we find a quantitative conversion within the polymer, concluding that two neighboring olefins always assume a relative geometry that allows them to form either of the diastereomers. A similar stereochemical behavior was recently observed in the [2 + 2]-photocycloaddition of cinnamic acids to α-truxillic acids.[26] Figure 2d shows six monomers that after polymerization will form the perimeter of a pore in the 2D polymer.

For an optimal polymerization, the wet monomer crystals were carefully placed in a sealed glass vial with residual mother liquor present. Irradiation was performed at approximately 4 °C by exposing this vial to a custom-built array of LEDs with maximum emission at λ = 530 nm (Figures S6 and S7, SI). This wavelength was chosen to be in the tail of the absorption spectrum. This "trick" is known to increase the homogeneity of scsc transformations.[21,27] Within a matter of minutes the color of the crystals changed from orange to yellow, indicating that the conjugation within the monomers was interrupted and polymerization has taken place [Figures 2e and S8 (SI)].

DOI: 10.1021/jacs.6b11857
J. Am. Chem. Soc. 2017, 139, 2053−2059

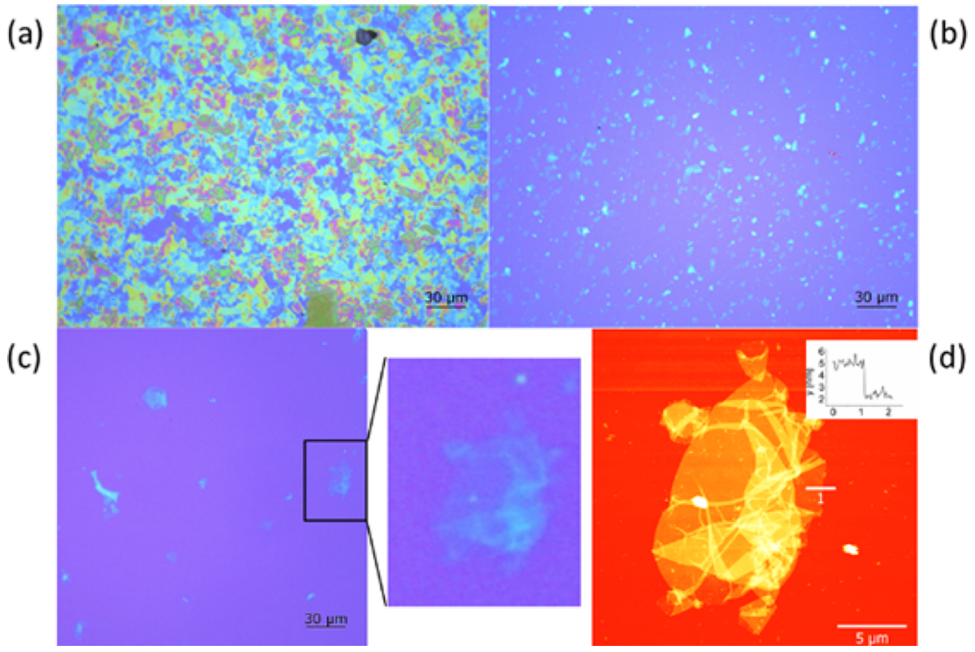

Figure 3. Exfoliation of the 2D polymer obtained from the photoirradiation of monomer **3**. OM images of drop-casted suspensions on 280 nm SiO_2/Si after 2 d (a) and 45 d (b) of exfoliation in GBL (As the exfoliation proceeds, the concentration of sheets increases. The dispersion in part b was therefore diluted to facilitate characterization). Spotting individual objects (c) after 6 d of exfoliation and scanning this very object with an AFM (height profile inserted) (d).

Ideally, a scsc transformation is proven by comparing monomer and polymer by XRD using the very same crystal. In the present case, this was not done because of the sensitivity of the monomer crystals, which required reducing their handling to the absolute minimum. The best polymer crystals were obtained by irradiating monomer crystals that were still covered with mother liquor and when handling was kept to a minimum. Solving the structure of polymerized crystals initially met with difficulties. For a detailed description, see chapter 1.7 of the SI. Data convergence was finally achieved by application of a disordered structure model assuming two diastereomeric states for the cyclobutane rings formed. Figures S9–S14 (SI) provide a reciprocal space reconstruction and several views of the packing of the polymer in the crystal. These two states [Figures 2f and S15 (SI)] are a direct consequence of the orientational sense of the olefins in the monomer crystal (Figures 2c,d). Their ratio is estimated to be blue:purple = 5:1 suggesting that the lattice decoration (i.e., the cyclobutane orientation on the lattice points) of the 2D polymer is not strictly trigonal but rather has to be seen as a mesh, the pores of which on average have five "blue" cyclobutanes and one "purple" cyclobutane. When looking at a single polymer layer along the *c*-axis (Figures S13 and S14, SI) one sees that there are pores with a size of 17 or 28 Å measuring the shortest and longest C–C distance in the same pore, respectively. All three distinguishable layers in the unit cell (Figure S10, SI) are slightly shifted relative to one another, meaning that the pores within each layer form channels with an effective diameter of about 5 Å throughout the entire crystal. This is a significant difference from a recent 2D polymer crystal from our laboratory, which does not have through-pores.[9b] Together with the volatility of the solvents used, these voids are the likely cause for the sensitivity of the monomer crystals. For the disorder of the *tert*-butyl groups, see Figure S16 (SI). The two kinds of disorder encountered in the polymer crystal cause very weak diffuse scattering features (Figure S17, SI).

Macroscopically, the polymer crystals stayed intact and even turned out to be much less sensitive toward the absence of solvent than the monomer crystals. This became evident during manipulation in the dry state, though now brittleness was observed. Successful scsc polymerization requires the reaction to take place with a minimum of volume change. Unfortunately, the exact volume change could not be measured because of the mentioned stability issue with the monomer crystals. The following cell parameters therefore refer to a starting situation with 25% polymerized monomer crystals [for monomer, space group $R\bar{3}$, a = 27.2214(12) Å, c = 16.1711(17) Å, V = 10377(1) Å^3; for polymer, space group $R\bar{3}$, a = 27.0482(6) Å, c = 16.1593(5) Å, V = 10238.4(5) Å^3] reflecting a volume contraction of the unit cells for the 75% remaining conversion of only 1.3%. Assuming a linear relation between conversion and unit cell changes, this value amounts to 2.9% for the entire process. Thus, the rather complex network formation can be largely accommodated within the available volume. We find this noteworthy, since attempts to prepare supposedly more simple linear polymers using analogous, difunctional styrylpyrylium salts only yielded oligomers, likely due to more severe changes in the cell parameters.[28]

Figure S10 (SI) shows the crystal structure of the 2D polymer obtained in a side view, and Figure 2g shows a top view of a single layer. Both of these representations refer to an idealized sheet with only one diastereomer present. For a general representation of a real sheet structure based on a random distribution of diastereomers, see Figure 2h. All close pairs of olefins have reacted to become the corresponding cyclobutanes, herewith establishing the structure of a novel 2D polymer. In the top view (Figure 2f), six pyrylium units point inside each pore; they are actually located above and below the polymer plane. Thus, each pore is decorated by a regular array

DOI: 10.1021/jacs.6b11857
J. Am. Chem. Soc. 2017, 139, 2053–2059

of six positively charged groups, which renders this macromolecule a 2D polyelectrolyte with a crystalline scaffold. The polymerization conversion was determined by IR and ^{13}C CP/MAS NMR spectroscopy (Figures S18 and S19, SI). Particularly indicative was the strong olefin IR vibration at 1585 cm^{-1} and the olefin signal in the NMR spectrum at δ = 150 ppm, which both disappeared virtually completely. Within the limits of resolution, this result was also confirmed by XRD.

Liquid phase exfoliations of fully polymerized crystals were carried out in several aprotic and polar solvents, such as DMSO, DMF, acetonitrile, and γ-butyrolactone (GBL), again using crystals with sizes of approximately 500 μm. GBL, a commonly used agent in liquid exfoliation of 2D materials,[16b,29a,b] gave the fastest exfoliation. However, to achieve the potentially enormous lateral extension of 2D polymers (theoretically up to the crystal size, e.g. 500 μm) not only fast exfoliation is desired but also a process gentle enough to not rupture the sheets too much. Clearly, this is a complicated matter and we cannot expand on it too much on the basis of the current knowledge. We rather describe one experiment, which allows one to draw the first meaningful conclusions. This refers to the use of only one crystal and its exposure to GBL at 80 °C over a period of 45 days. The use of one crystal avoids complications due to the dispersity in crystal size. Figure 3 shows important steps of this experiment. Parts a and b of Figure 3 refer to samples of the dispersion obtained from stirring the crystal in GBL at the given temperature for 2 and 45 days, respectively, both after drop-casting onto a 280 nm SiO_2/Si wafer.

While in Figure 3a the wafer is largely covered with sheets and sheet stacks with widely distributed thicknesses, the image in Figure 3b only exhibits sheets and sheet stacks with thicknesses well below 100 nm. This can be seen by the color change of the features in OM—a known, thickness-dependent phenomenon of 2D materials on SiO_2/Si wafers.[30] For another OM/AFM correlation, see Figure S20 (SI). While Figure 3 suggests that the exfoliation proceeds in the desired direction, these images have to be considered with care as they show small selected regions of the deposited material only. When deposited on solid substrates, much of the dispersed material deposits at the rim of the droplet during drying and dense agglomerates form which cannot meaningfully be analyzed (i.e., the "coffee-stain effect"). Consequently, the images in Figure 3 are not representative for the objects contained in the dispersion. Figure S21 (SI) shows an OM image of a larger part of the same wafer used in Figure 3a where the agglomerate is visible.[31]

Analysis of the dried features by optical microscopy provides three important insights. First, there are no features with lateral extensions anywhere near 500 μm. Second, there is a large dispersity in object thickness and object size, and third, there are occasionally very thin features. After 6 d of stirring at 80 °C in GBL, a sample of the resulting dispersion was drop-casted onto 280 nm SiO_2/Si, and countless, extremely thin features were observed by OM. The larger ones were spotted (Figure 3c) by their x,y-coordinates and then scanned by AFM in order to determine the apparent thickness (Figure 3d). The inset in Figure 3d provides a height profile typical for the investigated features [for more images and profiles, see Figure S22(SI)]. All these profiles uniformly show $h_{AFM} \approx 2.2 \pm 0.5$ nm. To exclude possible effects caused by the fact that the height is determined between two different materials, wafer and sheet, also step edges were analyzed, which resulted from sheets folded back on them. Such measurements gave the same approximate value. Considering the crystallographic sheet thickness of approximately h_{sc} = 1 nm (Figure S10, SI),[32] the value $h_{AFM} \approx 2.2 \pm 0.5$ nm suggests a double layer.[33,34] If one concentrates the search on objects with lateral extensions of approximately 1 μm and below, however, one finds many features that give $h_{AFM} \approx 1.2 \pm 0.5$ nm (Figure S23, SI). While mass fractions of thin sheets are not yet accessible, we conclude that wet exfoliation successfully provides access to large numbers of single- and double-layer sheets, whereby it appears that the double-layer features have the larger lateral dimensions.

Finally, we note that the 2D polymer upon thermal treatment at 150 °C undergoes retro-cycloaddition back to monomer, as judged by solution NMR spectroscopy (Figure S24, SI).

CONCLUSION AND OUTLOOK

This work presents the first single-crystal structure of a 2D polymer based on a topochemical [2 + 2]-cycloaddition and, thus, underlines the feasibility of the single-crystal approach to synthetic 2D polymers. This work also points toward a particularly facile exfoliation of the 2D polymer crystals down to a large number of features that are single and double sheets as judged by the AFM thicknesses of $h_{AFM} \approx 1.2 \pm 0.5$ and 2.2 ± 0.5 nm, respectively. There has always been high interest to investigate solution properties of synthetic 2D polymers, e.g., by scattering techniques.[35] This was so far hampered simply because of the lack of an appropriate system that would afford such solutions. Given the fact that the wet exfoliation presented here proceeds under mild conditions and provides a large number of extremely thin sheet stacks as well as single- and double-layer sheets and given the modern ultracentrifugation techniques,[36] it is reasonable to expect that fractions with sizable amounts of single- or double-layer sheets of 2D polymers will be available in the near future. This is where we see the greatest importance of the present work.

Furthermore, the XRD data analysis shows that the 2D polymer of monomer **3** has stereochemical diversity. On average, one of the six repeat units involved in the frame of each pore of the lattice is diastereomeric to the remaining five. In the absence of an indication for blockiness, we expect the distribution of the two diastereomeric forms to be random and the 2D polymer therefore to be *atactic* with a not strictly trigonal lattice. Whether this ratio is sensitive to the crystallization conditions is a fascinating issue yet to be explored.

A wet exfoliation experiment employing only one single crystal allows one to conclude that the sheets obtained have smaller lateral sizes than the crystal from which they are obtained.[37] It could not yet be clarified whether this is due to mosaicity in the crystal, phase transformations during polymerization, rupture events during exfoliation, or a mixture of all of these. Irrespective of what in the future will be discovered to be the cause, sheet sizes on the order of a few μm^2 refer to unprecedentedly high degrees of polymerization (1 μm^2 corresponds to P_n = 464 900 based on the XRD structure) which outperforms all linear polymerizations,[38] underlining the power of the chemistry reported. For small crystals, such an issue can in principle be approached by exfoliation of a polymerized single crystal after an appropriate edge decoration.[39] We note that currently it is not possible to provide a polydispersity for the sheet size but that the results reported mark steps toward such a goal. The classical concept of

DOI: 10.1021/jacs.6b11857
J. Am. Chem. Soc. 2017, 139, 2053−2059

polydispersity from linear solution polymerization might not apply.

■ ASSOCIATED CONTENT

Supporting Information

The Supporting Information is available free of charge on the ACS Publications website at DOI: 10.1021/jacs.6b11857.

Crystallography data for the 2D polymer in CIF format (CIF)

Crystallography data for the monomer in CIF format (CIF)

Additional information concerning the synthesis, crystallization, polymerization, X-ray analysis, IR, exfoliation, depolymerization, and AFM (PDF)

■ AUTHOR INFORMATION

Corresponding Author

*ads@mat.ethz.ch

ORCID

A. Dieter Schlüter: 0000-0001-9975-9831

Notes

The authors declare no competing financial interest.

■ ACKNOWLEDGMENTS

We thank Prof. Gerhard Wegner, MPI-P, Mainz, Germany, for helpful discussions and Drs. Alexei Mikheykin and Dmitry Chernyshov from SNBL at ESRF for their support during our experiments. We further thank Dr. Nils Trapp from the ETH Zurich Small Molecule Crystallography Center (SMoCC) and Dr. Václav Petříček from Fyzikální ústav Akademie věd, Czech Republic, for critically reviewing the crystal structures. We thank Dr. René Verel for the solid-state NMRs, Dr. Thomas Schweizer for the technical equipment, Prof. Nicholas D. Spencer for access to AFM, and Prof. Jan Vermant for access to OM. We thank Stan W. van de Poll for critically reading the manuscript.

■ REFERENCES

(1) (a) Mas-Ballesté, R.; Gómez-Navarro, C.; Gómez-Herrero, J.; Zamora, F. *Nanoscale* **2011**, *3*, 20−30. (b) Butler, S. Z.; Hollen, S. M.; Cao, L.; Cui, Y.; Gupta, J. A.; Gutiérrez, H. R.; Heinz, T. F.; Hong, S. S.; Huang, J.; Ismach, A. F.; Johnston-Halperin, E.; Kuno, M.; Plashnitsa, V. V.; Robinson, R. D.; Ruoff, R. S.; Salahuddin, S.; Shan, J.; Shi, L.; Spencer, M. G.; Terrones, M.; Windl, W.; Goldberger, J. E. *ACS Nano* **2013**, *7*, 2898−2926.

(2) (a) Bhimanapati, G. R.; Lin, Z.; Meunier, V.; Jung, Y.; Cha, J.; Das, S.; Xiao, D.; Son, Y.; Strano, M. S.; Cooper, V. R.; Liang, L.; Louie, S. G.; Ringe, E.; Zhou, W.; Kim, S. S.; Naik, R. R.; Sumpter, B. G.; Terrones, H.; Xia, F.; Wang, Y.; Zhu, J.; Akinwande, D.; Alem, N.; Schuller, J. A.; Schaak, R. E.; Terrones, M.; Robinson, J. A. *ACS Nano* **2015**, *9*, 11509−11539. (b) Lotsch, B. V. *Annu. Rev. Mater. Res.* **2015**, *45*, 85−109.

(3) (a) Fujita, M.; Kwon, Y. J.; Washizu, S.; Ogura, K. *J. Am. Chem. Soc.* **1994**, *116*, 1151−1152. (b) Biradha, K.; Domasevitch, K. V.; Moulton, B.; Seward, C.; Zaworotko, M. J. *Chem. Commun.* **1999**, 1327−1328. (c) Cheetham, A. K.; Rao, C. N. R.; Feller, R. K. *Chem. Commun.* **2006**, *46*, 4780−4795. (d) Kondo, M.; Furukawa, S.; Hirai, K.; Kitagawa, S. *Angew. Chem., Int. Ed.* **2010**, *49*, 5327−5330. (e) Zhang, M.; Feng, G.; Song, Z.; Zhou, Y.-P.; Chao, H.-Y.; Yuan, D.; Tan, T. T. Y.; Guo, Z.; Hu, Z.; Tang, B. Z.; Liu, B.; Zhao, D. *J. Am. Chem. Soc.* **2014**, *136*, 7241−7244.

(4) (a) Côté, A. P.; El-Kaderi, H. M.; Furukawa, H.; Hunt, J. R.; Yaghi, O. M. *J. Am. Chem. Soc.* **2007**, *129*, 12914−12915. (b) Ascherl, L.; Sick, T.; Margraf, J. T.; Lapidus, S. H.; Calik, M.; Hettstedt, C.; Karaghiosoff, K.; Döblinger, M.; Clark, T.; Chapman, K. W.; Auras, F.; Bein, T. *Nat. Chem.* **2016**, *8*, 310−316. (c) Smith, B. J.; Overholts, A. C.; Hwang, N.; Dichtel, W. R. *Chem. Commun.* **2016**, *52*, 3690−3693. (d) Xu, S.-Q.; Zhan, T.-G.; Wen, Q.; Pang, Z.-F.; Zhao, X. *ACS Macro Lett.* **2016**, *5*, 99−102.

(5) (a) Kuhn, P.; Antonietti, M.; Thomas, A. *Angew. Chem., Int. Ed.* **2008**, *47*, 3450−3453. (b) Bojdys, M. J.; Jeromenok, J.; Thomas, A.; Antonietti, M. *Adv. Mater.* **2010**, *22*, 2202−2205. (c) Ren, S.; Bojdys, M. J.; Dawson, R.; Laybourn, A.; Khimyak, Y. Z.; Adams, D. J.; Cooper, A. I. *Adv. Mater.* **2012**, *24*, 2357−2361.

(6) Sakamoto, J.; van Heijst, J.; Lukin, O.; Schlüter, A. D. *Angew. Chem., Int. Ed.* **2009**, *48*, 1030−1069.

(7) Payamyar, P.; King, B. T.; Ottinger, H. C.; Schlüter, A. D. *Chem. Commun.* **2016**, *52*, 18−34.

(8) (a) Stupp, S. I.; Son, S.; Lin, H. C.; Li, L. S. *Science* **1993**, *259*, 59−63. (b) Colson, J. W.; Dichtel, W. R. *Nat. Chem.* **2013**, *5*, 453−465. (c) Zhuang, X.; Mai, Y.; Wu, D.; Zhang, F.; Feng, X. *Adv. Mater.* **2015**, *27*, 403−427. (d) Baek, K.; Hwang, I.; Roy, I.; Shetty, D.; Kim, K. *Acc. Chem. Res.* **2015**, *48*, 2221−2229. (e) Boott, C. E.; Nazemi, A.; Manners, I. *Angew. Chem., Int. Ed.* **2015**, *54*, 13876−13894. (f) Cai, S.-L.; Zhang, W.-G.; Zuckermann, R. N.; Li, Z.-T.; Zhao, X.; Liu, Y. *Adv. Mater.* **2015**, *27*, 5762−5770. (g) Lackinger, M. *Polym. Int.* **2015**, *64*, 1073−1078. (h) Sakamoto, R.; Iwashima, T.; Tsuchiya, M.; Toyoda, R.; Matsuoka, R.; Kögel, J. F.; Kusaka, S.; Hoshiko, K.; Yagi, T.; Nagayama, T.; Nishihara, H. *J. Mater. Chem. A* **2015**, *3*, 15357−15371. (i) Zang, Y.; Aoki, T.; Teraguchi, M.; Kaneko, T.; Ma, L.; Jia, H. *Polym. Rev. (Philadelphia, PA, U. S.)* **2015**, *55*, 57−89. (j) Rodríguez-San-Miguel, D.; Amo-Ochoa, P.; Zamora, F. *Chem. Commun.* **2016**, *52*, 4113−4127. (k) Sakamoto, J.; Shinkai, S. *Kobunshi Ronbunshu* **2016**, *73*, 42−54.

(9) (a) Kissel, P.; Murray, D. J.; Wulftange, W. J.; Catalano, V. J.; King, B. T. *Nat. Chem.* **2014**, *6*, 774−778. (b) Kory, M. J.; Wörle, M.; Weber, T.; Payamyar, P.; van de Poll, S. W.; Dshemuchadse, J.; Trapp, N.; Schlüter, A. D. *Nat. Chem.* **2014**, *6*, 779−784.

(10) (a) Kissel, P.; Erni, R.; Schweizer, W. B.; Rossell, M. D.; King, B. T.; Bauer, T.; Götzinger, S.; Schlüter, A. D.; Sakamoto, J. *Nat. Chem.* **2012**, *4*, 287−291. (b) Bhola, R.; Payamyar, P.; Murray, D. J.; Kumar, B.; Teator, A. J.; Schmidt, M. U.; Hammer, S. M.; Saha, A.; Sakamoto, J.; Schlüter, A. D.; King, B. T. *J. Am. Chem. Soc.* **2013**, *135*, 14134−14141. (c) Wang, Z.; Randazzo, K.; Hou, X.; Simpson, J.; Struppe, J.; Ugrinov, A.; Kastern, B.; Wysocki, E.; Chu, Q. R. *Macromolecules* **2015**, *48*, 2894−2900.

(11) (a) Bauer, T.; Zheng, Z.; Renn, A.; Enning, R.; Stemmer, A.; Sakamoto, J.; Schlüter, A. D. *Angew. Chem., Int. Ed.* **2011**, *50*, 7879−7884. (b) Zheng, Z.; Ruiz-Vargas, C. S.; Bauer, T.; Rossi, A.; Payamyar, P.; Schütz, A.; Stemmer, A.; Sakamoto, J.; Schlüter, A. D. *Macromol. Rapid Commun.* **2013**, *34*, 1670−1680. (c) Chen, Y.; Li, M.; Payamyar, P.; Zheng, Z.; Sakamoto, J.; Schlüter, A. D. *ACS Macro Lett.* **2014**, *3*, 153−158. (d) Payamyar, P.; Kaja, K.; Ruiz-Vargas, C.; Stemmer, A.; Murray, D. J.; Johnson, C. J.; King, B. T.; Schiffmann, F.; VandeVondele, J.; Renn, A.; Götzinger, S.; Ceroni, P.; Schütz, A.; Lee, L.-T.; Zheng, Z.; Sakamoto, J.; Schlüter, A. D. *Adv. Mater.* **2014**, *26*, 2052−2058. (e) Payamyar, P.; Servalli, M.; Hungerland, T.; Schütz, A. P.; Zheng, Z.; Borgschulte, A.; Schlüter, A. D. *Macromol. Rapid Commun.* **2015**, *36*, 151−158. (f) Murray, D. J.; Patterson, D. D.; Payamyar, P.; Bhola, R.; Song, W.; Lackinger, M.; Schlüter, A. D.; King, B. T. *J. Am. Chem. Soc.* **2015**, *137*, 3450−3453.

(12) (a) Sakamoto, R.; Hoshiko, K.; Liu, Q.; Yagi, T.; Nagayama, T.; Kusaka, S.; Tsuchiya, M.; Kitagawa, Y.; Wong, W.-Y.; Nishihara, H. *Nat. Commun.* **2015**, *6*, 6713. (b) Takada, K.; Sakamoto, R.; Yi, S.-T.; Katagiri, S.; Kambe, T.; Nishihara, H. *J. Am. Chem. Soc.* **2015**, *137*, 4681−4689.

(13) Fan, Q.; Gottfried, J. M.; Zhu, J. *Acc. Chem. Res.* **2015**, *48*, 2484−2494.

(14) (a) Baek, K.; Yun, G.; Kim, Y.; Kim, D.; Hota, R.; Hwang, I.; Xu, D.; Ko, Y. H.; Gu, G. H.; Suh, J. H.; Park, C. G.; Sung, B. J.; Kim, K. *J. Am. Chem. Soc.* **2013**, *135*, 6523−6528. (b) Zhang, K.-D.; Tian, J.; Hanifi, D.; Zhang, Y.; Sue, A. C.-H.; Zhou, T.-Y.; Zhang, L.; Zhao, X.; Liu, Y.; Li, Z.-T. *J. Am. Chem. Soc.* **2013**, *135*, 17913−17918. (c) Xu,

DOI: 10.1021/jacs.6b11857
J. Am. Chem. Soc. 2017, 139, 2053−2059

S.-Q.; Zhang, X.; Nie, C.-B.; Pang, Z.-F.; Xu, X.-N.; Zhao, X. *Chem. Commun.* **2015**, *51*, 16417−16420. (d) Zhou, T.-Y.; Qi, Q.-Y.; Zhao, Q.-L.; Fu, J.; Liu, Y.; Ma, Z.; Zhao, X. *Polym. Chem.* **2015**, *6*, 3018−3023.
(15) Peplow, M. *Nature* **2016**, *536*, 266−268.
(16) (a) Hernandez, Y.; Nicolosi, V.; Lotya, M.; Blighe, F. M.; Sun, Z.; De, S.; McGovern, I. T.; Holland, B.; Byrne, M.; Gun'Ko, Y. K.; Boland, J. J.; Niraj, P.; Duesberg, G.; Krishnamurthy, S.; Goodhue, R.; Hutchison, J.; Scardaci, V.; Ferrari, A. C.; Coleman, J. N. *Nat. Nanotechnol.* **2008**, *3*, 563−568. (b) Coleman, J. N.; Lotya, M.; O'Neill, A.; Bergin, S. D.; King, P. J.; Khan, U.; Young, K.; Gaucher, A.; De, S.; Smith, R. J.; Shvets, I. V.; Arora, S. K.; Stanton, G.; Kim, H.-Y.; Lee, K.; Kim, G. T.; Duesberg, G. S.; Hallam, T.; Boland, J. J.; Wang, J. J.; Donegan, J. F.; Grunlan, J. C.; Moriarty, G.; Shmeliov, A.; Nicholls, R. J.; Perkins, J. M.; Grieveson, E. M.; Theuwissen, K.; McComb, D. W.; Nellist, P. D.; Nicolosi, V. *Science* **2011**, *331*, 568−571. (c) Hao, C.; Wen, F.; Xiang, J.; Yuan, S.; Yang, B.; Li, L.; Wang, W.; Zeng, Z.; Wang, L.; Liu, Z.; Tian, Y. *Adv. Funct. Mater.* **2016**, *26*, 2016−2024.
(17) (a) Wegner, G. *Makromol. Chem.* **1971**, *145*, 85−94. (b) Nakanishi, H.; Hasegawa, M.; Sasada, Y. *J. Polym. Sci., Part A-2: Polym. Phys.* **1972**, *10*, 1537−1553. (c) Wegner, G. *Pure Appl. Chem.* **1977**, *49*, 443−454. (d) Hasegawa, M. *Chem. Rev.* **1983**, *83*, 507−518.
(18) (a) Toh, N. L.; Nagarathinam, M.; Vittal, J. J. *Angew. Chem., Int. Ed.* **2005**, *44*, 2237−2241. (b) Yamada, S.; Uematsu, N.; Yamashita, K. *J. Am. Chem. Soc.* **2007**, *129*, 12100−12101. (c) Yamada, S.; Tokugawa, Y. *J. Am. Chem. Soc.* **2009**, *131*, 2098−2099. (d) Briceno, A.; Hill, Y.; Gonzalez, T.; Diaz de Delgado, G. *Dalton Trans.* **2009**, 1602−1610. (e) Linares, M.; Briceno, A. *New J. Chem.* **2010**, *34*, 587−590.
(19) (a) Desiraju, G. R. *Crystal Engineering: The Design of Organic Solids*; Elsevier: Amsterdam, 1989. (b) Desiraju, G. R. *J. Am. Chem. Soc.* **2013**, *135*, 9952−9967.
(20) Servalli, M.; Trapp, N.; Woerle, M.; Klärner, F. G. *J. Org. Chem.* **2016**, *81*, 2572−2580.
(21) Novak, K.; Enkelmann, V.; Wegner, G.; Wagener, K. B. *Angew. Chem., Int. Ed. Engl.* **1993**, *32*, 1614−1616.
(22) Hesse, K.; Hünig, S. *Liebigs Ann. Chem.* **1985**, *1985*, 715−739.
(23) Enkelmann, V.; Wegner, G.; Novak, K.; Wagener, K. B. *J. Am. Chem. Soc.* **1993**, *115*, 10390−10391.
(24) Such conversions are determined by XRD. A partially converted monomer crystal is represented as the weighted average electron density of monomer and polymer. For the technical details including systematic errors, see the following: (a) Watkin, D. *J. Appl. Crystallogr.* **2008**, *41*, 491−522. (b) Mueller, P. *Crystallogr. Rev.* **2009**, *15*, 57−83.
(25) Schmidt, G. M. J. *Pure Appl. Chem.* **1971**, *27*, 647−678.
(26) Fernandes, M. A.; Levendis, D. C. *CrystEngComm* **2016**, *18*, 7363−7376.
(27) Enkelmann, V.; Wegner, G.; Novak, K.; Wagener, K. B. *J. Am. Chem. Soc.* **1993**, *115*, 10390−10391.
(28) Buchholz, V.; Enkelmann, V. *Mol. Cryst. Liq. Cryst. Sci. Technol., Sect. A* **2001**, *356*, 315−325.
(29) (a) Hernandez, Y.; Nicolosi, V.; Lotya, M.; Blighe, F. M.; Sun, Z.; De, S.; McGovern, I. T.; Holland, B.; Byrne, M.; Gun'Ko, Y. K.; Boland, J. J.; Niraj, P.; Duesberg, G.; Krishnamurthy, S.; Goodhue, R.; Hutchison, J.; Scardaci, V.; Ferrari, A. C.; Coleman, J. N. *Nat. Nanotechnol.* **2008**, *3*, 563−568. (b) Hao, C.; Wen, F.; Xiang, J.; Yuan, S.; Yang, B.; Li, L.; Wang, W.; Zeng, Z.; Wang, L.; Liu, Z.; Tian, Y. *Adv. Funct. Mater.* **2016**, *26*, 2016−2024.
(30) Li, H.; Wu, J.; Huang, X.; Lu, G.; Yang, J.; Lu, X.; Xiong, Q.; Zhang, H. *ACS Nano* **2013**, *7*, 10344−10353.
(31) Furthermore, there is a suspicion that exfoliation under the chosen conditions for 45 d might be too harsh. Large-scale OM images reveal in addition to sheets also features that look like irregular networks, the origin and molecular structure of which are yet unknown. Our present research therefore concentrates on less demanding conditions.
(32) The thickness of molecular sheets is difficult to define, as continuum models do not apply. The value of 1 nm results when measuring the distance between two of the outermost *tert*-butyl groups on both sides of the sheet. If, however, the height of the unit cell is divided by 3, to account for the three sheets per cell, the value h = 0.54006(6) nm is obtained. This (too) low value is a result of the geared arrangement between consecutive layers through which the *tert*-butyl groups of one layer penetrate into the pores of the neighboring layers.
(33) There are several effects that contribute to AFM height determinations under ambient conditions which can cause overestimations. For example, see the following: Gibaja, C.; Rodriguez-San-Miguel, D.; Ares, P.; Gómez-Herrero, J.; Varela, M.; Gillen, R.; Maultzsch, J.; Hauke, F.; Hirsch, A.; Abellán, G.; Zamora, F. *Angew. Chem., Int. Ed.* **2016**, *55*, 14345−14349.
(34) (a) Ziegler, D.; Rychen, J.; Naujoks, N.; Stemmer, A. *Nanotechnology* **2007**, *18*, 225505. (b) Nemes-Incze, P.; Osváth, Z.; Kamarás, K.; Biró, L. P. *Carbon* **2008**, *46*, 1435−1442. (c) Paton, K. R.; Varrla, E.; Backes, C.; Smith, R. J.; Khan, U.; O'Neill, A.; Boland, C.; Lotya, M.; Istrate, O. M.; King, P.; Higgins, T.; Barwich, S.; May, P.; Puczkarski, P.; Ahmed, I.; Moebius, M.; Pettersson, H.; Long, E.; Coelho, J.; O'Brien, S. E.; McGuire, E. K.; Sanchez, B. M.; Duesberg, G. S.; McEvoy, N.; Pennycook, T. J.; Downing, C.; Crossley, A.; Nicolosi, V.; Coleman, J. N. *Nat. Mater.* **2014**, *13*, 624−630. (d) Hanlon, D.; Backes, C.; Doherty, E.; Cucinotta, C. S.; Berner, N. C.; Boland, C.; Lee, K.; Harvey, A.; Lynch, P.; Gholamvand, Z.; Zhang, S.; Wang, K.; Moynihan, G.; Pokle, A.; Ramasse, Q. M.; McEvoy, N.; Blau, W. J.; Wang, J.; Abellan, G.; Hauke, F.; Hirsch, A.; Sanvito, S.; O'Regan, D. D.; Duesberg, G. S.; Nicolosi, V.; Coleman, J. N. *Nat. Commun.* **2015**, *6*, 8563. (e) Wagner, T.; Beyer, H.; Reissner, P.; Mensch, P.; Riel, H.; Gotsmann, B.; Stemmer, A. *Beilstein J. Nanotechnol.* **2015**, *6*, 2193−2206.
(35) (a) Payamyar, P.; King, B. T.; Öttinger, H. C.; Schlüter, A. D. *Chem. Commun.* **2016**, *52*, 18−34. (b) Schlüter, A. D.; Payamyar, P.; Öttinger, H. C. *Macromol. Rapid Commun.* **2016**, *37*, 1638−1650.
(36) Planken, K. L.; Cölfen, H. *Nanoscale* **2010**, *2*, 1849−1869.
(37) The rhomboedric 2D polymer crystals have the point group $\bar{3}$; therefore, the *c*-axis runs parallel to the long diagonal through the crystal. The individual 2D polymers are oriented perpendicular to the *c*-axis, which results in an intrinsic sheet size distribution. This distribution encompasses tiny sheets from regions near the two crystal vertices, through which the *c*-axis passes, to large sheets, which are from regions near the center of the *c*-axis, right where the crystal has its largest extension in the *a*,*b*-direction.
(38) McIntyre, D.; Fetters, L. J.; Slagowski, E. *Science* **1972**, *176*, 1041−1043.
(39) Zhao, Y.; Bernitzky, R. H. M.; Kory, M. J.; Hofer, G.; Hofkens, J.; Schlüter, A. D. *J. Am. Chem. Soc.* **2016**, *138*, 8976−8981.

DOI: 10.1021/jacs.6b11857
J. Am. Chem. Soc. 2017, 139, 2053−2059